Nanoscale particle motion reveals polymer mobility gradient in nanocomposites

Erkan Senses[1], Suresh Narayanan[2], Antonio Faraone[3]

[1]Department of Chemical and Biological Engineering, Koç University, Istanbul 34450, Turkey

[2]Advanced Photon Source, Argonne National Laboratory, Argonne, Illinois 60439, USA

[3]NIST Center for Neutron Research, Gaithersburg, Maryland 20899, USA

KEYWORDS. Nanoparticle dynamics, interface, interphase, polymer nanocomposites, bound polymer

ABSTRACT: Polymer mobility near nanoparticle surfaces has been extensively discussed, however, direct experimental observation in the nanocomposite melts has been a difficult task. Here, by taking advantage of large dynamical asymmetry between miscible matrix and surface-bound polymers, we highlighted their interphases and studied the resulting effect on the nanoparticle relaxation using x-ray photon correlation spectroscopy. The local mobility gradient is signified by an unprecedented increase in the relaxation time at length scales on the order of polymer radius of gyration. The effect is accompanied by a transition from simple diffusive to subdiffusive behavior in accord with viscous and entangled dynamics of polymers in the matrix and in the interphase, respectively. Our results demonstrate that the nanoparticle-induced polymer mobility changes in the interphases of nanocomposite melts can be extracted from the length-scale-dependent slow particle motion itself.

Dynamics at nanoparticle (NP)-polymer interfaces is linked to the unusual rheological properties of polymer nanocomposites (PNCs) [1-3]; the details of such correlation is not well-understood. Polymers confined in thin film geometries display structure and dynamics that can be very different from the bulk [4-6]. Similarly, favorable polymer-nanoparticle interaction immobilize the chains on NP surfaces [7] and form a confined interfacial layer accompanied by a transition phase (*i.e.* interphase) with a mobility gradient towards the bulk. Despite utmost importance for both fundamental physics and engineering, the transport properties of advanced nanocomposite materials, as well as the spatial extent and the complex dynamics of the interphases are not well known.

Various techniques have, therefore, been employed. For example, Cheng *et al*.[8] used atomic force microscopy to visualize the interfacial layer in glassy PNCs (in which the NPs are immobilized) and Brillion light scattering revealed the elastic modulus of polymer twice larger at the ≈ 2 to 3 nm thick interface compared to the bulk. In the melt state, however, direct observation of the changes in the polymer dynamics in the vicinity of mobile NPs is an extremely difficult task. Conventional techniques, such as dielectric and mechanical spectroscopy [9-11], lack appropriate spatial resolution, thus, providing polymer behavior averaged from the bulk and the interphase, which requires a detailed modeling and assumptions. On the other hand, high resolution neutron spectroscopy (specifically quasielastic backscattering) allows direct observation of the segmental dynamics in nanocomposite melts. It was shown that attractive interaction between polymer and NPs slows down the overall segmental dynamics in nanocomposite melts [12]. The length-scale of quasielastic neutron spectroscopy is yet restricted to very short distances (typically below several nm's) and the time scale is rather fast (typically faster than ns) [13] compared to the longest relaxation time of the polymers, which essentially controls the viscosity. Therefore, a direct link between the modified segmental dynamics and the spatial variation of the polymer mobility within the interphases has not been possible.

Here, we used x-ray photon correlation spectroscopy (XPCS) and investigated the slow NP relaxation, instead of that of the polymer, at timescales from a few hundred milliseconds to tens of seconds. Since the NP motion is essentially directed by the local polymer viscosity, we hypothesize that the polymer mobility gradient (if there is any) around the NPs can be decoded from the NP dynamics itself.

We considered two nanocomposite systems: (i) SiO_2 NPs dispersed in a low-T_g poly(ethylene oxide) (PEO, $T_{g,PEO} \approx$ 210 K), representing a model attractive PNC system, (ii) SiO_2 NPs coated with a high-T_g poly(methyl methacrylate) (PMMA, $T_{g,PMMA} \approx$ 400 K) and dispersed in the low-T_g PEO matrix. In the latter, PEO and PMMA form a neutral interface since the Flory-Huggins parameter is negligibly small [14]. The large T_g-difference between them enhances the viscosity contrast between the interface and matrix, and al-

lowed us to identify, for the first time, the mobility gradient around NPs from the length-scale dependent NPs relaxation.

The hydrogenated PEO (*h*-PEO, M_w=35 kg/mol, M_w/M_n=1.08) was purchased from Polymer Source Inc. Deuterated PEO (*d*-PEO, M_w=35 kg/mol, M_w/M_n=1.09) and *h*-PMMA (M_w=98.5 kg/mol, M_w/M_n=1.08) were purchased from Sigma-Aldrich. Both polymers are well-above the entanglement molar masses (2 kg/mol for PEO and 18 kg/mol for PMMA [15]). The polymers were dried further under vacuum at 363 K for 12 h prior to use. The colloidal silica NPs (≈ 25 nm in radius with size polydispersity ≈ 0.3) in methyl ethyl ketone were supplied by Nissan Chemicals America and used as received. The PNCs were prepared according to the protocol described elsewhere [16]. The PNCs with PMMA coated NPs were prepared using a protocol similar to bare NP PNC preparation. The final NP concentration was determined from thermogravimetric analysis to be 4 % and 5 % (by volume), corresponding to face-to-face interparticle distances (IDs) of 67 and 75 nm for the bare NPs and the PMMA coated NPs, respectively. Note that the radius of gyration, R_g , of 35 kg/mol PEO melt is ≈ 6.8 nm [15] - ten times smaller than the IDs.

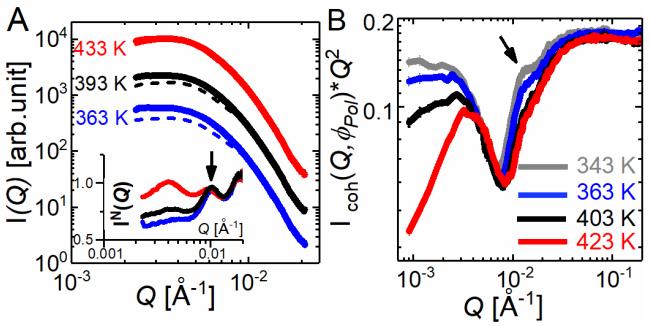

Figure. 1. (A). SAXS profiles (shifted vertically for clarity) from the PNCs at different temperatures. The symbols are for PNCs with bare NPs and the lines are for PNCs with PMMA coated NPs. The inset shows the deviations of the profiles obtained by dividing the SAXS intensities of the coated particles by the bare NPs, $I^N(Q)$. (B). Temperature dependent Kratky plots from the SANS profiles of the PMMA coated NPs in PEO matrix that is contrast matched to the NPs. The arrow in SAXS and SANS indicate the location of the bound layer correlations.

In both PNC samples, the presence of a bound polymer layer (BL), either PEO or PMMA, provides steric protection against NP aggregation. The SAXS data in Figure 1A shows no low-Q upturn in the intensity confirming aggregate-free dispersion of both bare NPs (shown as lines) and PMMA-coated NPs (shown as symbols) in PEO matrices. There is a clear difference between the profiles at intermediate and low-*Q*, which we display in the inset by dividing the intensity from the coated NPs by the intensity of the bare NPs, $I^N(Q)$. The peak at $Q \approx 0.01$ Å^{-1} corresponds to a length-scale ≈ 60 nm -close to NP diameter- and can be due to the PMMA BL which has different electron density than the matrix PEO. Notice also that the location of the peak is essentially temperature independent, however, the deviations of the profiles from the bare NPs and PMMA coated NPs at low *Q* become smaller at elevated temperatures. This suggests an enhanced intermixing of PEO and PMMA at elevated temperatures which reduces the x-ray contrast between the BL and the matrix.

The BL correlation peaks are more apparent in small-angle neutron scattering (SANS) [17] which we performed at NG30B beamline at National Institute of Standards and Technology Center for Neutron Research (NIST-NCNR). We minimized the particle contribution to scattering intensity in the intermediate and high-*Q* by using a mixture of *d*-PEO and *h*-PEO (*d*/*h*: 52/48 ratio) matrix that matches with the scattering length density of SiO_2 nanoparticles; the *h*-PMMA BL is therefore highlighted. The details of the SANS experiments and analysis are given in Supporting Information. Figure 1B shows the Kratky plot (IQ^2 vs. *Q*) for the *h*-PMMA coated NPs in the contrast matched matrix. At high *Q*, the intensity is due to the PEO chains which shows the usual Debye-plateau. At intermediate and low-*Q*, the contribution from *h*-PMMA interfacial layer results in a correlation peak at $Q \approx 0.01$ Å^{-1}, similar to the SAXS result. Its intensity appears to significantly decrease with temperature, and, at T = 423 K, results in a profile that is similar to the bare NP composites where the BL is less visible (see the profiles for the neat and the PMMA coated NPs in Supporting Information). This suggest a decrease of scattering contrast within the interphases due to enhanced mixing of *h*-PMMA with *d*/*h* PEO chains with temperature, as SAXS data also suggested and in parallel with the thermal-stiffening nature of these nanocomposites [16, 18].

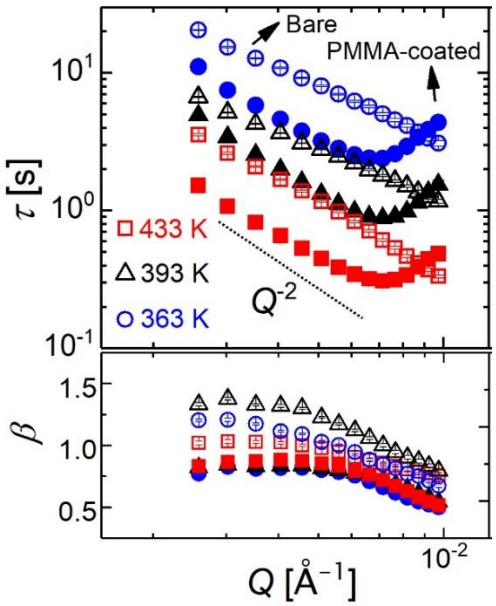

Figure. 2. Relaxation times (τ) and stretching exponents (β) for bare NPs (shown by open symbols) and PMMA-coated NPs (shown by filled symbols) at different temperatures. The line shows the scaling of the relaxation time with the wave-vector for a simple diffusive motion (*i.e.* $\tau \propto Q^{-2}$). Similar results are obtained for the average relaxation time

$\langle\tau\rangle=(\tau/\beta)\Gamma(1/\beta)$, Γ being the gamma function, as shown in the SI.

We then looked at the slow NP motion which is directed by the local viscosity of the medium. We performed XPCS experiments on beamline 8-ID-I at the Advanced Photon Source at Argonne National Laboratory. The normalized intensity-intensity auto-correlation function, $g_2(Q,t)$, was obtained over the wave vector range 0.003 Å^{-1} < Q < 0.02 Å^{-1} corresponding to the length-scale ≈ (20-200) nm. The correlation function is related to the intermediate scattering function (ISF), $f(Q,t)$, as $g_2(Q,t) \sim 1 + A[f(Q,t)]^2$, with A and t being the Siegert factor of the instrument and the delay time, respectively. The correlation functions at all length-scales for bare NPs and PMMA-coated NPs in PEO at 393 K are shown in Supplemental Materials. The g_2s for the bare NPs is nearly exponential and the relaxation time monotonically decreases with increasing Q, as expected. In contrast, the behavior of the PMMA-coated NPs is non-monotonic: at low-Q it behaves similar to bare NPs and at higher Q, the relaxation becomes remarkably stretched with the timescale shifted to longer values.

To gain further insight, the ISF was best fit to the stretched/compressed exponential functions, $f(Q,t) = \exp[-(t/\tau)^{\beta}]$, with relaxation time, τ, and the stretching/compressing exponent, β. Figure 2 shows the bare NPs exhibit diffusive motion with $\tau \propto Q^{-2}$ scaling with β above and close to unity and move faster at higher temperatures. Diffusive motion for bare NPs is expected. In a previous work, Guo *et al.* [19] showed that the tracer NPs in unentangling polystyrene melt exhibit simple diffusion at T> 1.2 T_g whereas hyperdiffusive motion was observed at lower T close to the T_g of the matrix. Since the longest relaxation time of PEO at the experimental temperatures (T> 1.7 T_g, PEO) falls well below the shortest XPCS time (t_{XPCS}> 10 ms > t_d, where t_d is the terminal relaxation time [16]), the entanglements of PEO are relaxed and the particle motion is directed by the bulk viscous motion of the matrix, therefore, NPs exhibit simple diffusion.

The non-monotonic relaxation of PMMA coated NPs in the same PEO matrix is apparent in the Q dependence of τ and β. At large distances (low Q), the scaling $\tau \propto Q^{-2}$ and $\beta \approx 1$ suggests that these NPs also exhibit simple diffusion in the PEO matrix similar to the bare NPs. The diffusive motion holds up to $Q \approx 0.007$ Å^{-1} (corresponding length-scales around 90 nm) above which τ monotonically increases with Q. As the length-scale probed gets shorter, the NPs feel the effect of the less-mobile interfacial PMMA layer. This is clearly different from the behavior of bare NPs; the observed stiffening at the nanoscale is clearly due to the mobility gradient induced by the bound PMMA layer. To our best knowledge, such an unusual NP relaxation has not been observed before. The increase in τ with Q is accompanied by the decrease of β. The stretched exponential relaxation, $\beta < 1$, at high-Q is a signature of a sub-diffusive NP motion which is dictated by the entanglements in polymeric liquids , as previously shown by Guo *et al.* [20] and Poling-Skutvit *et al.* [21]. As mentioned earlier, the entanglements are relaxed (in the time-scale of XPCS) for the PEO matrix, however, the entanglement relaxation time for PMMA is extremely long (hundreds of seconds) around its T_g, therefore, the NP motion gets increasingly sub-diffusive as shorter length-scales are probed.

The temperature dependent SAXS and SANS profiles suggested an enhanced intermixing of PEO matrix with interfacial PMMA at elevated temperatures. The transition between the matrix-dominated and the interphase-controlled regions gets broader with less strong upturn of τ at 433 K (above $T_{g,PMMA}$). Note, however, that the stretching exponent for PMMA coated NPs is not significantly affected by temperature; the NP motion is still governed by the entangled dynamics within interphases at high Q and at all T investigated.

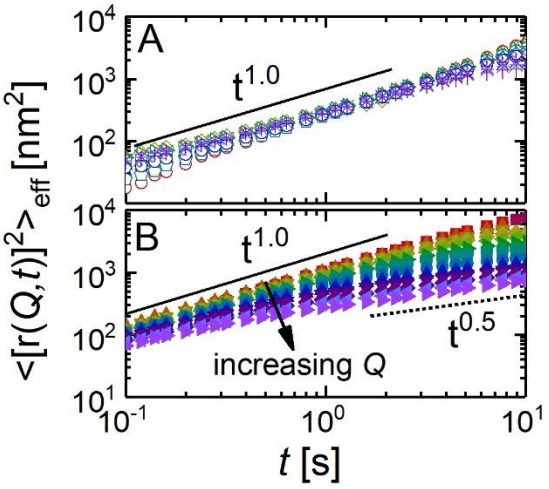

Figure. 3. Relative effective mean square displacements, $\langle[r(Q,t)]^2\rangle_{eff}$, as a function of time for (A) the bare NPs and (B) for the PMMA coated NPs at different Q values at 363 K.

The length-scale dependent NP mobility can be more quantitatively evaluated from the mean-square displacements (MSD). As the XPCS signal is collective in nature, the probed dynamics is related to the relative motion of the NPs with respect to each other; however, at Q values above the first structure factor peak, i.e. for length scales smaller than the interparticle distance, the dynamics probed is mostly the single particle one. Therefore, the ISF can be related to a relative effective, Q and t dependent, MSD_{eff} by $f(Q,t) = exp\left(-\frac{\langle[r(Q,t)]^2\rangle_{eff}}{6}Q^2\right)$ within the Gaussian approximation [21]. Figure 3 compares $\langle[r(Q,t)]^2\rangle_{eff}$ for the bare and the PMMA coated NPs in PEO at 363 K. The scaling $\langle[r(Q,t)]^2\rangle_{eff} \sim t^{1.0}$ is a signature of diffusive behavior and holds for the bare NPs for all Q whereas it applies for the PMMA coated NPs only at low-Q. When increasing Q for the PMMA coated NP, MSD transition from $\approx t^{1.0}$ towards $\approx t^{0.5}$ scaling; characteristic of subdiffusive motion becomes more apparent at longer times.

At the low-Q regime of Figure 2, the calculated viscosity values from the XPCS relaxation time and using the Stokes-Einstein relation, $\eta_{XPCS} = k_B T/[6\pi D_{eff}(Q \to 0)R_{NP}]$, with an effective diffusion coefficient defined as $D_{eff}(Q) = 1/[\tau(Q)/Q^2]$, are close to the bulk viscosity of PEO [22] for the bare NPs. The temperature dependence of the local viscosity is also well-described by Vogel-Fulcher-Tamman (VFT) equation, $\eta(T) = \eta_o \exp[B/(T - T_\infty)]$ with known B = 1090 and T_o = 155 K for bulk PEO [22-23] (shown in Figure 4A). The attractive bare NPs, therefore, do not affect the properties of the matrix polymer away from the interface. Starr *et* al. [24] reached a similar conclusion from their theoretical study on strongly attractive polymer nanocomposites which indicated that the BL 'cloaks' nanoparticles, hence, the dynamics of the matrix remains unaffected. This is in contrast to PMMA-coated NPs at low Q, where the calculated local viscosities are ≈ 2 times lower than the bulk viscosity of PEO (Fig. 4A). We attribute this to negligible enthalpic interaction between the PMMA layer and PEO matrix; the PMMA-coated NPs essentially create neutral interfaces for PEO matrix which is akin to free surfaces. In their XPCS work, Koga *et al.* [25] showed the free surface of thin films to be less entangled than the bulk chains. Similar to this argument, the PEO can be disentangled in the presence of well-dispersed neutral/repulsive interfaces, which in this case resulted in a two-fold decrease in the viscosity experienced by the PMMA-coated NPs. This is in line with the disentanglement of PEO matrix chains in presence of PMMA interfacial layer observed in neutron spin-echo in a previous work. [16].

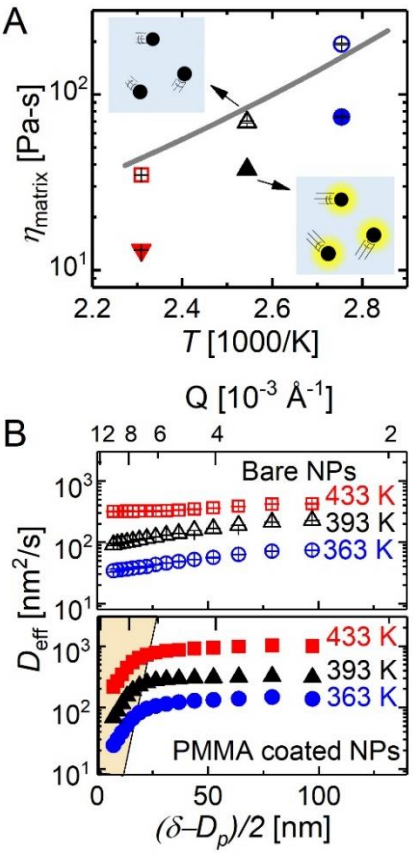

Figure. 4. (A) Temperature dependence of the matrix viscosity experienced by the NPs at low-Q. The open and filled symbols are for the bare NPs and the PMMA coated NPs, respectively. The line is the VFT prediction for the neat PEO. The inset images illustrate the motion of NPs with and without PMMA layer. (B) The effective diffusion coefficient for the bare NPs and the PMMA-coated NPs as a function of the length-scale probed relative to the NP size.

In the high Q regime where the interphase effects dominate, the estimation of viscosity from sub-diffusive motion is not readily possible. Instead, we compared the Q-dependence of the effective diffusion coefficient. Figure 4B shows D_{eff} as a function of the probed length scale, $\delta = 2\pi / Q$ relative to the particle size (D_p), representing the distance from the NP surface. The mobility gradient around the PMMA coated NPs is clear. At short distances, D_{eff}'s are lower by nearly an order of magnitude and tend to converge as high-T_g PMMA interface layer is approached. The measurement temperature has pronounced effect on the plateau region and the transition from interphase to the bulk gets broader with temperature. At 363 K, the transition occurs over a length-scale ≈ 20 nm, a distance ≈ 2 times larger than R_g of PMMA, whereas at 433 K, the transition is broader ≈ 40 nm, corresponding to a distance that is ≈ 4 times larger than $R_{g,PMMA}$. Previous studies on the nanoparticle dynamics and chain diffusion also inferred that the effect of attractive interfaces can propagate to distances as large as 8 R_g of the bulk chains [26-28]. In contrast to the PMMA coated NPs, the mobility gradient for the bare NPs in the neat PEO matrix is not appreciable well above the T_g of the PEO.

The results clearly showed that functionalization of the NP surfaces with a high-T_g polymer that is miscible with the low-T_g matrix enhanced the viscosity contrast between the interfacial and the bulk chains and allowed to access the mobility gradients. It is noteworthy here that we considered particle sizes larger than the chain size (and entanglement mesh size) ($R \approx 25$ nm >>$R_g \approx 7$ nm); therefore, the recent discussions on the NP size effect [29-31] are not relevant in this work and the observed dynamical changes are due to interfaces only. We believe, however, that using smaller NPs would allow accessing mobility gradients even closer to NPs surfaces, provided that the size effects are carefully taken into account. Furthermore, our matrix polymer was well-above the T_g in the liquid state with no entanglement effects. This study can be extended to higher T_g polymer matrices so that the interface effects on the dynamic heterogeneities associated with the glass transition can also be extracted from hyperdiffusive relaxation of NPs. [32-33] Also, as the interphase is strongly dependent on the polymer conformation on NPs, we conjecture that the effect of polymer grafting on the degree of interfacial entanglements and the mobility gradients within the graft layer [34] can also reflect on the slow NP dynamics. In all cases, though, individual dispersion of NPs in polymers, either in melt state or solution, is essential to eliminate any contribution from particle caging or morphological effects.[35-36]

In conclusion, we investigated the slow motion of well-dispersed nanoparticles in polymer melts using XPCS. The mobility gradient around NPs is reflected as an entanglement controlled sub-diffusive motion with characteristic relaxation time increasing with decreasing probed-length scales. The small-angle scattering and the temperature dependent NP dynamics demonstrated that the long-debated questions on the dynamics and the spatial extent of the interphases in polymer nanocomposite melts can be well-studied from the length-scale-dependent NP motion. We conjecture that our results will stimulate new theoretical and experimental studies concerning the polymer dynamics near nanoparticle surfaces that is linked to the macroscopic rheological properties of advanced nanocomposites.

ASSOCIATED CONTENT

Supporting Information. SANS intensity profiles and representative correlation plots are provided. This material is available free of charge via the Internet at http://pubs.acs.org.

AUTHOR INFORMATION

Corresponding Author

* esenses@ku.edu.tr

Author Contributions

The manuscript was written through contributions of all authors.

ACKNOWLEDGMENT

This work utilized facilities supported in part by the National Science Foundation under Grant No. DMR-1508249 and used resources of the Advanced Photon Source, a U.S. Department of Energy (DOE) Office of Science User Facility operated for the DOE Office of Science by Argonne National Laboratory under Contract No. DE-AC02-06CH11357. The identification of any commercial product or trade name does not imply endorsement or recommendation by the National Institute of Standards and Technology. Throughout the paper error bars represent one standard deviation.

REFERENCES

1. Holt, A. P.; Griffin, P. J.; Bocharova, V.; Agapov, A. L.; Imel, A. E.; Dadmun, M. D.; Sangoro, J. R.; Sokolov, A. P., Dynamics at the Polymer/Nanoparticle Interface in Poly(2-vinylpyridine)/Silica Nanocomposites. *Macromolecules* **2014,** *47*, 1837-1843.
2. Sternstein, S. S.; Zhu, A.-J., Reinforcement Mechanism of Nanofilled Polymer Melts As Elucidated by Nonlinear Viscoelastic Behavior. *Macromolecules* **2002,** *35*, 7262-7273.
3. Krutyeva, M.; Wischnewski, A.; Monkenbusch, M.; Willner, L.; Maiz, J.; Mijangos, C.; Arbe, A.; Colmenero, J.; Radulescu, A.; Holderer, O.; Ohl, M.; Richter, D., Effect of Nanoconfinement on Polymer Dynamics: Surface Layers and Interphases. *Phys. Rev. Lett.* **2013,** *110*, 108303.
4. Ramanathan, T.; Abdala, A. A.; Stankovich, S.; Dikin, D. A.; Herrera-Alonso, M.; Piner, R. D.; Adamson, D. H.; Schniepp, H. C.; Chen, X.; Ruoff, R. S.; Nguyen, S. T.; Aksay, I. A.; Prud'Homme, R. K.; Brinson, L. C., Functionalized graphene sheets for polymer nanocomposites. *Nat. Nanotechnol.* **2008,** *3*, 327.
5. Napolitano, S.; Sferrazza, M., How irreversible adsorption affects interfacial properties of polymers. *Adv. Colloid Interface Sci.* **2017,** *247*, 172-177.
6. Koga, T.; Li, C.; Endoh, M. K.; Koo, J.; Rafailovich, M.; Narayanan, S.; Lee, D. R.; Lurio, L. B.; Sinha, S. K., Reduced Viscosity of the Free Surface in Entangled Polymer Melt Films. *Phys. Rev. Lett.* **2010,** *104*, 066101.
7. Harton, S. E.; Kumar, S. K.; Yang, H.; Koga, T.; Hicks, K.; Lee, H.; Mijovic, J.; Liu, M.; Vallery, R. S.; Gidley, D. W., Immobilized Polymer Layers on Spherical Nanoparticles. *Macromolecules* **2010,** *43*, 3415-3421.
8. Cheng, S.; Bocharova, V.; Belianinov, A.; Xiong, S.; Kisliuk, A.; Somnath, S.; Holt, A. P.; Ovchinnikova, O. S.; Jesse, S.; Martin, H.; Etampawala, T.; Dadmun, M.; Sokolov, A. P., Unraveling the Mechanism of Nanoscale Mechanical Reinforcement in Glassy Polymer Nanocomposites. *Nano Lett.* **2016,** *16*, 3630-3637.
9. Carroll, B.; Cheng, S.; Sokolov, A. P., Analyzing the Interfacial Layer Properties in Polymer Nanocomposites by Broadband Dielectric Spectroscopy. *Macromolecules* **2017,** *50*, 6149-6163.
10. Berriot, J.; Montes, H.; Lequeux, F.; Long, D.; Sotta, P., Evidence for the Shift of the Glass Transition near the Particles in Silica-Filled Elastomers. *Macromolecules* **2002,** *35*, 9756-9762.
11. Mortazavian, H.; Fennell, C. J.; Blum, F. D., Structure of the Interfacial Region in Adsorbed Poly(vinyl acetate) on Silica. *Macromolecules* **2016,** *49*, 298-307.
12. Senses, E.; Tyagi, M.; Natarajan, B.; Narayanan, S.; Faraone, A., Chain dynamics and nanoparticle motion in attractive polymer nanocomposites subjected to large deformations. *Soft Matter* **2017,** *13*, 7922-7929.
13. Higgins, J. S.; Benoît Henri. Polymers and Neutron Scattering; Oxford Series on Neutron Scattering in Condensed Matter, 8; Clarendon Press: Oxford, **1994**.
14. Ito, H.; Russell, T. P.; Wignall, G. D., Interactions in mixtures of poly(ethylene oxide) and poly(methyl methacrylate). *Macromolecules* **1987,** *20*, 2213-2220.
15. Fetters, L.; Lohse, D.; Colby, R., Chain dimensions and entanglement spacings. In *Physical properties of polymers handbook*, Springer: 2007; pp 447-454.
16. Senses, E.; Faraone, A.; Akcora, P., Microscopic Chain Motion in Polymer Nanocomposites with Dynamically Asymmetric Interphases. *Sci. Rep.* **2016,** *6*, 29326.
17. Sen, S.; Xie, Y.; Kumar, S. K.; Yang, H.; Bansal, A.; Ho, D. L.; Hall, L.; Hooper, J. B.; Schweizer, K. S., Chain Conformations and Bound-Layer Correlations in Polymer Nanocomposites. *Phys. Rev. Lett.* **2007,** *98*, 128302.
18. Senses, E.; Isherwood, A.; Akcora, P., Reversible Thermal Stiffening in Polymer Nanocomposites. *ACS Appl. Mater. Interfaces* **2015,** *7*, 14682-14689.
19. Guo, H.; Bourret, G.; Corbierre, M. K.; Rucareanu, S.; Lennox, R. B.; Laaziri, K.; Piche, L.; Sutton, M.; Harden, J. L.; Leheny, R. L., Nanoparticle Motion within Glassy Polymer Melts. *Phys. Rev. Lett.* **2009,** *102*, 075702.
20. Guo, H.; Bourret, G.; Lennox, R. B.; Sutton, M.; Harden, J. L.; Leheny, R. L., Entanglement-Controlled Subdiffusion of Nanoparticles within Concentrated Polymer Solutions. *Phys. Rev. Lett.* **2012,** *109*, 055901.
21. Poling-Skutvik, R.; Mongcopa, K. I. S.; Faraone, A.; Narayanan, S.; Conrad, J. C.; Krishnamoorti, R., Structure and Dynamics of Interacting Nanoparticles in Semidilute Polymer Solutions. *Macromolecules* **2016,** *49*, 6568-6577.

22. Senses, E.; Ansar, S. M.; Kitchens, C. L.; Mao, Y.; Narayanan, S.; Natarajan, B.; Faraone, A., Small Particle Driven Chain Disentanglements in Polymer Nanocomposites. *Phys. Rev. Lett.* **2017,** *118*, 147801.

23. Niedzwiedz, K.; Wischnewski, A.; Pyckhout-Hintzen, W.; Allgaier, J.; Richter, D.; Faraone, A., Chain Dynamics and Viscoelastic Properties of Poly(ethylene oxide). *Macromolecules* **2008,** *41*, 4866-4872.

24. Starr, F. W.; Douglas, J. F.; Meng, D.; Kumar, S. K., Bound Layers "Cloak" Nanoparticles in Strongly Interacting Polymer Nanocomposites. *ACS Nano* **2016,** *10*, 10960-10965.

25. Lin, C.-C.; Gam, S.; Meth, J. S.; Clarke, N.; Winey, K. I.; Composto, R. J., Do Attractive Polymer–Nanoparticle Interactions Retard Polymer Diffusion in Nanocomposites? *Macromolecules* **2013,** *46*, 4502-4509.

26. Tung, W.-S.; Griffin, P. J.; Meth, J. S.; Clarke, N.; Composto, R. J.; Winey, K. I., Temperature-Dependent Suppression of Polymer Diffusion in Polymer Nanocomposites. *ACS Macro Lett.* **2016,** *5*, 735-739.

27. Senses, E.; Narayanan, S.; Mao, Y.; Faraone, A., Nanoscale Particle Motion in Attractive Polymer Nanocomposites. *Phys. Rev. Lett.* **2017,** *119*, 237801.

28. Cheng, S.; Xie, S.-J.; Carrillo, J.-M. Y.; Carroll, B.; Martin, H.; Cao, P.-F.; Dadmun, M. D.; Sumpter, B. G.; Novikov, V. N.; Schweizer, K. S.; Sokolov, A. P., Big Effect of Small Nanoparticles: A Shift in Paradigm for Polymer Nanocomposites. *ACS Nano* **2017,** *11*, 752-759.

29. Carroll, B.; Bocharova, V.; Carrillo, J.-M. Y.; Kisliuk, A.; Cheng, S.; Yamamoto, U.; Schweizer, K. S.; Sumpter, B. G.; Sokolov, A. P., Diffusion of Sticky Nanoparticles in a Polymer Melt: Crossover from Suppressed to Enhanced Transport. *Macromolecules* **2018,** *51*, 2268-2275.

30. Grabowski, C. A.; Mukhopadhyay, A., Size Effect of Nanoparticle Diffusion in a Polymer Melt. *Macromolecules* **2014,** *47*, 7238-7242.

31. Hoshino, T.; Murakami, D.; Tanaka, Y.; Takata, M.; Jinnai, H.; Takahara, A., Dynamical crossover between hyperdiffusion and subdiffusion of polymer-grafted nanoparticles in a polymer matrix. *Phys. Rev. E* **2013,** *88*, 032602.

32. Wei, Y.; Xu, Y.; Faraone, A.; Hore, M. J. A., Local Structure and Relaxation Dynamics in the Brush of Polymer-Grafted Silica Nanoparticles. *ACS Macro Lett.* **2018,** *7*, 699-704.

33. Liu, S.; Senses, E.; Jiao, Y.; Narayanan, S.; Akcora, P., Structure and Entanglement Factors on Dynamics of Polymer-Grafted Nanoparticles. *ACS Macro Lett.* **2016,** *5*, 569-573.

34. Brambilla, G.; El Masri, D.; Pierno, M.; Berthier, L.; Cipelletti, L.; Petekidis, G.; Schofield, A. B., Probing the Equilibrium Dynamics of Colloidal Hard Spheres above the Mode-Coupling Glass Transition. *Phys. Rev. Lett.* **2009,** *102*, 085703.

Table of Contents use only